coatings

Article

Feasibility Study on Biodegradable Black Paper-Based Film Solidified Using Cooked Tung Oil

Yi Wu [1,2,*], Yicheng Shi [1,3], Yudie Zhao [1,3] and Yu Yin [1,3]

1 Department of Civil Aviation Safety Engineering, Civil Aviation Flight University of China, Guanghan 618307, China
2 CAAC Academy, Civil Aviation Flight University of China, Guanghan 618307, China
3 Civil Aircraft Fire Science and Safety Engineering Key Laboratory of Sichuan Province, Civil Aviation Flight University of China, Guanghan 618307, China
* Correspondence: wuyi@cafuc.edu.cn

Abstract: New biodegradable paper-based films are a hot research topic in the development of green agriculture. In this study, a black paper-based film coated with cooked tung oil with excellent mechanical properties, a hydrophobic surface, high heat transfer and strong weather resistance was prepared by spraying high-pigment carbon black solution on the surface of base paper. The results showed that the surface-solidified oil film had a rough structure produced via the brush coating process using cooked tung oil. The base film of the black paper had a given hydrophobic structure, and the contact angle reached 98.9°. Cooked tung oil permeates into the inside of the paper base, and after curing, it forms a multi-dimensional network film structure. The maximum tensile stress of the black paper base film is about 123% higher than that of the original paper base film. The coloring of carbon black gives the black paper base film a heat conduction effect, and the average heat transfer rate reaches 15.12 °C/s. Cooked tung oil is combined with the paper-based fiber high-toughness layer to form a stable system. The existence of a cured film improves the basic mechanics and hydrophobicity, and the resistance to ultraviolet radiation and hot air is greatly improved. This study provides a feasible scheme for the application of a black paper base film coated with cooked tung oil.

Keywords: black mulch film; degradable paper mulch film; hydrophobicity; heat transfer; anti-aging

Citation: Wu, Y.; Shi, Y.; Zhao, Y.; Yin, Y. Feasibility Study on Biodegradable Black Paper-Based Film Solidified Using Cooked Tung Oil. *Coatings* **2024**, *14*, 284. https://doi.org/10.3390/coatings14030284

Academic Editors: Antonella Salvini and Eduardo Guzmán

Received: 28 December 2023
Revised: 6 February 2024
Accepted: 7 February 2024
Published: 26 February 2024

1. Introduction

Plastic film mulching can effectively improve soil temperature, reduce soil mechanical resistance, increase microbial biomass, maintain soil organic components, maintain the nutrients needed by crops and efficiently increase the yield [1–4]. Population growth has increased competition for soil, food and water resources. Especially in some arid and semi-arid areas, furrow and ridge mulching with plastic film is an important way to improve grain yield [5]. However, the insufficient recycling of traditional plastic films is the main factor leading to plastic pollution [6]. Since the mass production of plastic products began in the 1950s, plastic residues have forced many countries around the world to expend a lot of manpower and financial resources to reduce the pollution caused by plastics [7,8]. To solve this problem, biodegradable films are used in research and development roles to replace traditional plastic films [9]. Nowadays, there are many raw materials for the production of biodegradable films, such as polysaccharides, starch, cellulose, biological derivative monomers, microorganisms and so on [10]. Harada [11] et al. used PBAT, polylactic acid and natural fillers (carbon black, organic fertilizer and silica rice ash) to prepare biodegradable mulch film and studied its biodegradability in simulated soil. The results show that the biodegradable film with a natural filler is superior to the biodegradable film with a pure mixture.

The colors of plastic films are diverse, and black plastic films have excellent water retention abilities. However, their low light transmittance leads to insufficient light entering the soil under the film, thus inhibiting the growth of weeds. Brown et al. [12] compared the growth and yield of sweet pepper under four conditions: bare soil (BS), bare soil–drip irrigation (BS–DI), black plastic film (BPM) and black plastic film–drip irrigation (BMP–DI). The results showed that the yield of sweet pepper increased by 57.1% and 63.1%, respectively, under BMP and BMP–DI conditions. M.J. Kasperbauer [13] found a way to increase the yield of strawberries in the seedbed cultivation of strawberries through the use of a black plastic film. The yield of strawberries covered with red plastic and standard black plastic was compared. The results showed that the far-red light and red light reflected by red plastic affected the distribution of photosynthate mediated by photosensitivity, making strawberries larger when using a red plastic film, and photosensitivity directly acted on fruit development, showing an advantage in terms of yield. Anzalone [14] et al. conducted a three-year field experiment on tomato using several different biodegradable plastic film materials, such as rice straw, barley straw, corn residue, wormwood, black biodegradable plastic, kraft paper, PE, herbicide, artificial weeding and no weeding. The weed control effect of these materials instead of black polyethylene mulch film was studied. The experiments showed that the best weed control effect is paper. For most crops, weeds will seize soil, oxygen, organic matter, etc., in the early growth process [15]. Therefore, the use of black plastic films undoubtedly reduces the production cost of crops and improves weeding efficiency.

As a reinforcing raw material, carbon black has a low cost, can be used as a dye and has good stability and high thermal conductivity [16]. It is widely used in lithium batteries, capacitors, composite rubber, etc. [17–20]. Mishra et al. [21] added 2.5% low-load carbon black nano powder (CBNP) to improve the thermal conductivity and photothermal conversion efficiency of organic phase change materials (PCMs) by 135% and 84%. Leong [22] et al. used carbon black dispersion based on polyethylene glycol (PEG) or di (ethylene glycol) butyl ether and dissolved ethyl cellulose to provide a thermal interface material that is superior to solder. The results showed that carbon black was superior to materials with higher thermal conductivity (graphite, diamond and nickel particles and carbon filaments) in providing high-performance thermal paste, and it is superior to solder in providing high thermal contact conductivity.

Pure tung oil is processed from tung oil. Compared with raw tung oil, pure tung oil is easier to solidify and form a smooth film, which has good heat resistance and corrosion resistance [23–25]. It can be used for color fixing, furniture maintenance, machine repair instead of using clear oil, etc. [26]. Tung oil is widely used to modify materials. Huang [27] et al. used tung oil to react with maleic anhydride (MA) and then reacted it with hydroxyethyl acrylate (HEA) or triacrylate (PETA) and methacrylate (GMA) to synthesize UV-curable resin. The results show that the successful preparation of the target resin depends on the feed ratio of MA, tung oil and HEA (or PETA). The higher the carbon bond content of acrylate, the faster the curing rate and the lower the carbon bond conversion rate. All of the cured films have good thermal stability, and the transformation range is 40–52 °C. Wang [28] et al. prepared nine kinds of mixtures by adding hemp fiber into tung oil lime mud. The basic mechanical properties, pore structure, surface morphology and characterization of the cured and aged slurry were tested. The results show that the fiber addition reaction will strengthen the composite and accelerate the carbonation process of lime. The curing process enhances the compressive strength of the cured pulp. The composite with 1.0% fiber and 5% tung oil has a good frost resistance cycle and salt resistance.

The research progress of degradable plastic films is gradually maturing, but there is no paper-based film that can really be applied in current research. In this study, a new type of black paper base film covered with cooked tung oil was prepared by using degradable base paper base film, combining the process of spraying carbon black solution and brushing cooked tung oil. In order to evaluate the practicability of black paper-based film, the mechanical strength was judged using a basic mechanical test, the hydrophobic property of surface technology was evaluated via the static water contact angle, and its stability was judged through a weather resistance experiment (ultraviolet aging and dry heat aging).

The results of the heat conduction experiment provided an answer for solving the low light transmittance of black film. The preparation technology of paper-based film has been widely studied in the past. However, in this study, carbon black and cooked tung oil were used to enhance the strength of paper-based film, and the applicable black paper-based film with excellent comprehensive performance was prepared by using low-cost raw materials and simple technology, which provided an efficient and environmentally friendly path for preparing stable and reliable black plastic film and a new scheme for promoting global green agriculture.

2. Materials and Methods

2.1. Experimental Materials and Equipment

The materials and equipment were purchased from the following companies: High-pigment carbon black: Hengnan Chemical Products Co., Ltd. (Zhengzhou, China); high-quality cooked tung oil: Gushi County, China Fangji tung oil processing plant, Gushi County, Henan Province, China, specific gravity (20 °C) 0.938, refractive index (20 °C) 1.519; fully biodegradable paper-based film (BM), developed by Tottori Prefecture, Tottori City, Japan; deionized water: self-made in laboratory; anhydrous ethanol: 95% purity, Fuyu Chemical Co., Ltd, Tianjin, China; microcomputer-controlled electronic universal testing machine (WDW–10M): Jinan Zhongluchang Testing Machine (Jinan, China); contact angle tester (Theta Flex): Baolin Scientific, (Shanghai, China); ultraviolet accelerated weathering test chamber (MU3089): China Shanghai Moujing Industrial Co., Ltd. (Shanghai, China); hot air aging testing machine (MU3040C): Shanghai Moujing Industrial Co., Ltd., (Shanghai, China); interferometric three-dimensional surface topography instrument (ZeGage): ZYGO, Inc., Middlefield, CT, USA; infrared thermal imager (Tis60+): Fluke, Evered, WA, USA; field-emission scanning electron microscope (NOVA NanoSEM450): FEI Company, Hillsboro, OR, USA; infrared spectrometer (IRTracer-100): Shimadzu, Kyoto, Japan.

2.2. Preparation of Black Paper-Based Film

Figure 1 shows the preparation process of black paper base. Thus, 150 mL of deionized water was added to 1.5 g of water-soluble carbon black and the mixture stirred to prepare 1% carbon black solution. We used an oil-free compressor to spray the carbon black solution evenly on the front and back surfaces of the base paper, and let it dry for 20 min at room temperature. After the carbon black completely adheres to the surface of the base paper, we brushed the cooked tung oil on the front and back surfaces of the base paper to ensure uniform brushing. The samples brushed with cooked tung oil were dried in an oven at 100 °C for 4 h, and the cooked tung oil solidified on the surface of the paper base; finally, the black paper base film covered with cooked tung oil was prepared.

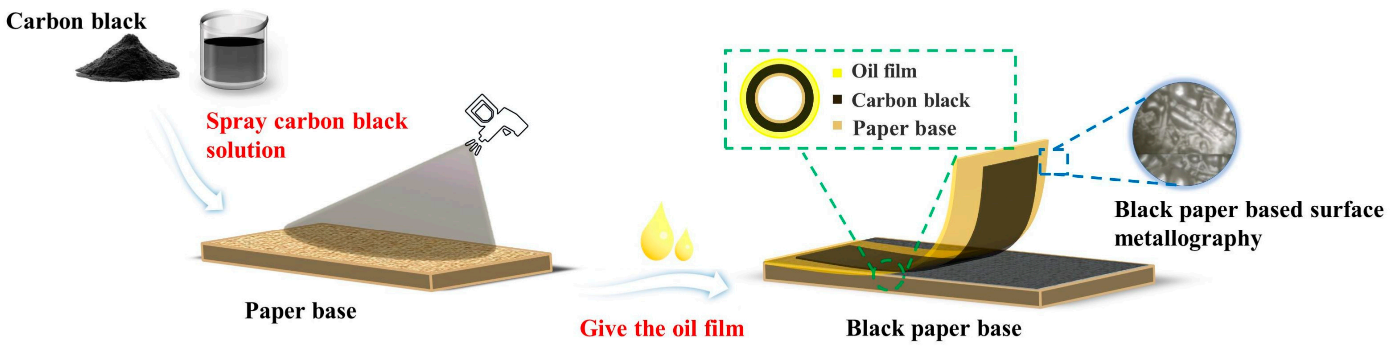

Figure 1. Preparation process of black paper mulch film.

3. Results and Discussions

3.1. Surface Morphology Analysis

In the SEM test, the accelerated voltage (EHT) of the paper-based membrane measurement is set to 5 KV, and the accelerated voltage of cooked tung oil is set to 20 KV. The working distance (WD) between them is between around 6.7 mm and 7.2 mm, and the magnification depends on the presentation state of different samples. In the EDS test, the Amp time is 3.84 µs, magnification (Mag) is set to 250 and EHT is set to 20 KV. Figure 2a,b show the SEM analysis of water-soluble high-pigment carbon black and cooked tung oil. The carbon black powder aggregates, and the particles are aggregated. This characteristic means there is a good effect in the coloring stage of the paper-based film. Looking at Figure 2b, there are some bubbles on the surface of cooked tung oil. After the surface of the sample is brushed and dried, the air inside the bubbles is released during the drying process. Therefore, during the curing process, the cooked tung oil will form a rough surface structure of the black paper base film, as shown in Figure 2f. Figure 2c,e characterize the cross-section of the black paper base film by SEM and EDS. The left side of the section boundary is black paper base, and the right side is base paper base. With the dividing line as the center line, the left and right collinear length are swept by 950 mm. Figure 2e shows the surface element changes of different paper base surfaces. On both sides of the dividing line, compared with the black paper covered with oil film, the base paper on the right side has a larger change range of the Ca element and a higher change frequency of the C element. According to the differences between two kinds of paper-based film elements and the distribution of C, O and N in Figure 2e,g,h, the production process for a black paper-based film coated with an oil film is feasible. Figure 2d is a two-dimensional Fourier-transform infrared spectrum analysis of base paper and black paper. The FT–IR recording range was 4000 to 1000 cm^{-1} with a resolution of 2 cm^{-1}. In the base paper, there is a characteristic peak of stretching vibration of the –OH-associated group in the infrared spectrum near 3270 cm^{-1}, and there is a broad peak of the symmetric stretching vibration of $–CH_3$ and $–CH_2$ groups between 2853 cm^{-1} and 2875 cm^{-1}. There is a strong absorption peak of –C–O–C and C–OH at 1029 cm^{-1}. There is a characteristic peak of $–CH_2–$ antisymmetric stretching vibration at 2925 cm^{-1}. There are $–CH_3$, $–CH_2–$ antisymmetric stretching and symmetric bending vibration peaks near 1459 cm^{-1}. There is a characteristic peak of –CO– (lipid) expansion at 1735 cm^{-1}. The disappearance of the characteristic peak of the −OH group on the surface of the black paper base membrane indicates that the cooked tung oil is completely covered on the surface of the black paper base membrane, and the existence of fatty groups further proves that the cooked tung oil is closely attached to the surface of the black paper base film.

3.2. Mechanical Properties

In the practical application of a plastic film, its mechanical strength is a key component. In the process of spreading and using a plastic film, it will be affected by wind, rain, weeds and some destructive external forces. Therefore, the mechanical strength of mulch film determines whether a mulch film can be applied. According to the standard GB/T22898-2008 [29], basic mechanical tests for membrane samples on base paper and black paper were carried out by using an electronic universal testing machine controlled by a microcomputer. According to the standard GB/T1040.3-2006 [30], the samples were cut into dumbbell-shaped tensile samples of 115 mm $\times$ 25 mm and right-angle tear samples of 100 mm $\times$ 20 mm, and tensile and tear tests were carried out, respectively. The experimental speed was 100 mm/min, and it was repeated five times. Figure 3b,c clearly show that there is an oil film attached to the surface of the black paper base film, which tightly covers and wraps the base paper fibers. Paper fiber itself is a network structure cross-linked with wood fibers. It is a combination of fibers formed by glue adhesion. In the basic mechanical test of a paper base film, as shown in Figure 3d,e, the maximum tensile and tearing force of black paper base film is greatly improved compared with that of the original paper base film. The maximum tensile force increased by 123.2%, and the maximum tearing force increased by 69.59%. From Figure 3f, as a whole, the mechanical strength of the black paper base film is larger than that of the original paper base film, whether in the tensile test or tear test. This is mainly due to the solidified oil film formed by cooked tung oil on the surface of the black paper base film. With the curing process of cooked tung oil in a drying oven, its oil molecules cross-link with each other to form a dense complex structure. It adheres to the surface of the paper base and improves the mechanical endurance of the black paper base film [31,32]. Figure 3g,h show more clearly that the fibers of the base paper crisscross each other and the tightness of the solidified oil film on the surface of the paper coated with cooked tung oil. A shown in Figure 3i, the paper base is soaked in oil during the brushing process of cooked tung oil. The cooked tung oil permeates between the paper fibers, and after drying and curing, the fiber-cooked tung oil–fibers interweave with each other to produce a strong pulling force. Compared with the fiber–fiber structure of the base paper, the existence of cooked tung oil undoubtedly endows the black paper base film with excellent mechanical strength, and the mechanism is higher than that of the base paper.

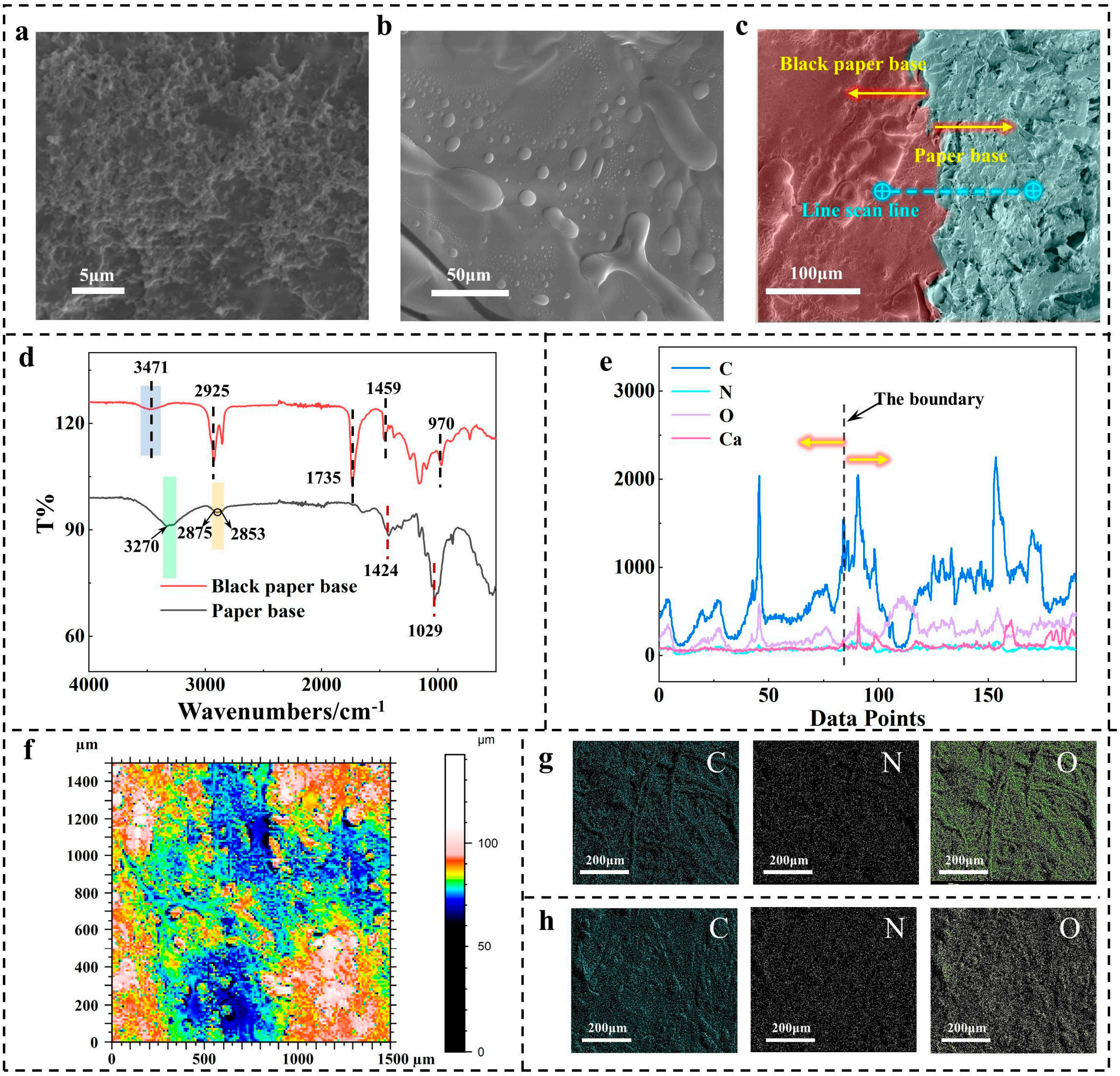

Figure 2. Surface analysis: (**a**) water-soluble pigment carbon black SEM; (**b**) SEM of cooked tung oil; (**c**) SEM of black paper mulch film section; (**d**) infrared spectrum analysis of base paper and black paper base film (different colors represent different characteristic peaks); (**e**) EDS of black paper mulch film section (the left and right arrows represent the parts of the black paper base and base paper base film, respectively); (**f**) false color view of black paper base film surface; (**g**) EDS on the film surface of base paper; (**h**) EDS on the surface of black paper base film.

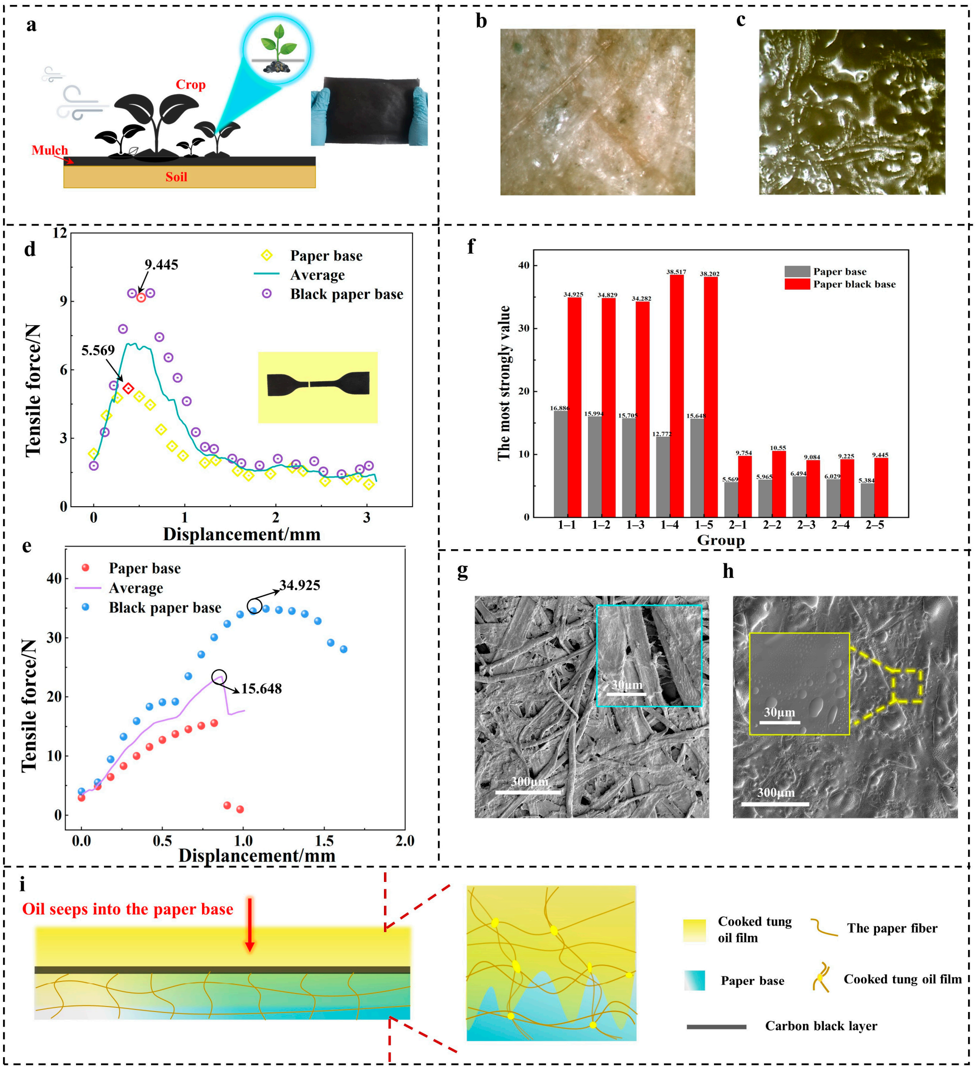

Figure 3. Mechanical test and mechanism analysis (**a**) simulates the use of plastic film in natural environment; (**b**) metallographic image of base film of base paper; (**c**) metallographic image of black paper base film; (**d**) stretching–displacement curves of film on base paper and black paper; (**e**) tear–displacement curve of film on base paper and black paper; (**f**) maximum tensile and tearing force of paper base film; (**g**) base paper SEM (the upper-right corner is further enlarged); (**h**) black paper-based SEM; (**i**) schematic diagram of action mechanism of cooked tung oil (the dashed lines point to the model cross-section).

3.3. Hydrophobic Property

Crops must cope with a changing environment in the production process. Among them, rainwater is an important environmental condition in the early growth of crops. In the paper-forming stage, the fibers are crisscrossed, and the fibers are dry and tough. However, when water permeates the paper, the fiber absorbs water and expands, and the fiber web structure becomes soft and broken. Therefore, rotting in water is a significant defect of paper-based films.

A contact angle weighing instrument was used to test the hydrophobicity of the base paper and black paper base films. In this study, the static contact angle is used to evaluate the hydrophobic properties of paper-based films. The steps are as follows: Cut the paper base to a width of 1 cm and place it on a glass slide. Measure the static contact angle. Select five points randomly on the surface of the paper base. Drop 4 μL of deionized water on the surface of the paper-based sample. The change characteristics of the static contact angle were measured. Figure 4a shows the manufacturing process of the black paper base film coated with cooked tung oil. Brush coating of the cooked tung oil on the surface of the base paper is equivalent to a protective layer, which makes the hydrophilic paper base film transition to a hydrophobic black paper base film. Figure 4b,c show that the surface of the base film of base paper is extremely hydrophilic. In the static contact angle test, when the liquid drops are on the film surface of the base paper, they gradually wet the base paper. As can be seen from Figure 4c, within 20 s, the droplet volume gradually decreases, and the paper fibers absorb water and expand. Finally, the base paper is completely soaked by liquid droplets. Figure 4h,I show that, after the water droplets are dropped onto the surface of the black paper base film, the contact angle is stable around 97.9° (>90°), showing hydrophobicity. The water drops are still on the surface, and the black paper base is not soaked, keeping its original state.

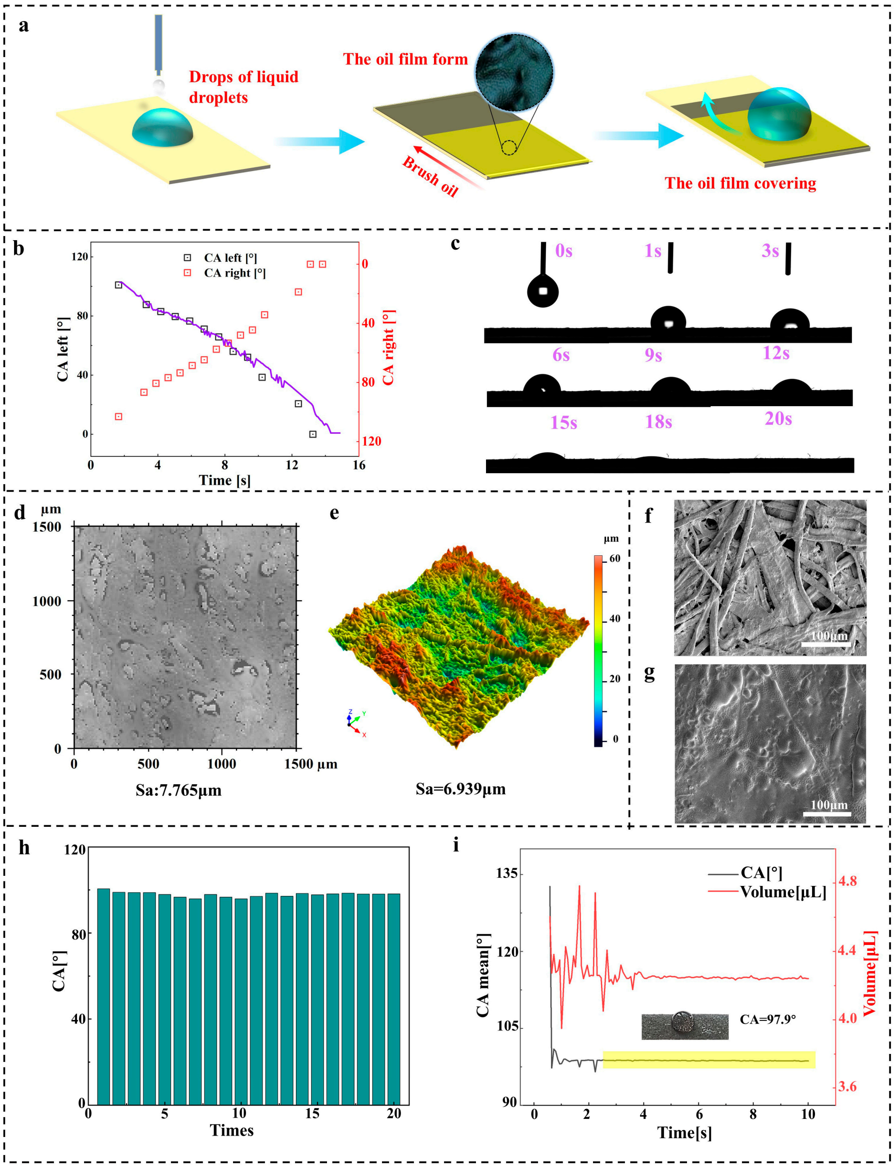

Figure 4. Discussion on hydrophobic properties of paper base film. (**a**) Schematic diagram of the process from hydrophilic base paper base film to hydrophobic black paper base film; (**b**) change in static contact angle of base paper film droplets during infiltration (purple lines show CA changes); (**c**) actual change in contact angle of liquid droplets on the surface of base paper; (**d**) black paper base film step height view; (**e**) 3D view of the film surface of base paper; (**f**) base paper SEM; (**g**) SEM of black paper base film; (**h**) contact angle test of black paper base film; (**i**) change in static contact angle of black paper base film (yellow highlights the smoothness of the curve).

The main factor to realize the hydrophilicity of base paper to the hydrophobicity of a black paper base film is the solidification of cooked tung oil. After spraying carbon black solution on the surface of the base paper and brushing with a layer of cooked tung oil, the surface of the base paper is obviously hydrophobic. Figure 4d,e show the rough surface morphology of the black paper base film and base paper, respectively. The arithmetic average height Sa of the base paper surface is 6.939 μm. The surface roughness of the black paper base Sa = 7.765 μm, which is 11.9% higher than that of the base film of base paper. Cooked tung oil, as a kind of drying oil, can be crosslinked with oxygen during drying. In this way, the surface of the black paper base is brushed with cooked tung oil. During the curing process, the cooked tung oil on the surface of the black paper base is partially separated from the paper base sprayed with carbon black, and some wrinkles appear in the oil film; the bubbles generated during the brushing process of tung oil may burst, resulting in the surface of the black paper base becoming rough and losing its original luster [33]. Figure 4f,g compare the SEM of two kinds of paper-based films. The surface wrinkles of black paper-based films are obvious, and the appearance of a micro-rough structure realizes the surface hydrophobicity of black paper-based films.

3.4. Efficient Heat Transfer Performance

The thermal conductivity of a black paper-based film was studied. The sample of the paper-based film was used as a medium at room temperature. We heated the heating plate (self-made in the laboratory) to 60 °C. The paper sample was cut to 5 cm × 5 cm and placed on the heating plate, and we monitored the heating process of the paper surface with an infrared thermal imager. Due to the low thickness of the paper film itself, it is difficult to grasp its temperature change in time. A small amount of cylindrical silica gel was placed on the paper base, and the time of its temperature rise to 60 °C was monitored using an infrared thermal imager; then, the heat transfer effects of different paper-based films were compared. Figure 5a shows that, after the heating plate is heated to 60 °C, the paper-based sample is placed. When the thermometer detects that the surface temperature of the paper-based sample reaches 60 °C, place a silica gel block to monitor its temperature change. Figure 5b shows that when the silica gel block on the surface of the base paper is initially placed, the temperature is 32.42 °C, and the time point is 22 s. After that, the time points of the silica gel block at about 40 °C, 45 °C, 55 °C and 60 °C were recorded, and the heat transfer rate was calculated. When the base paper is the heat transfer medium, the time for the silica gel block to rise to 45.08 °C and 60.05 °C is 35 s and 220 s, respectively. The heat transfer rates are 36.17 °C/s and 12.6 °C/s, respectively. Obviously, the temperature rise rate decreases in the stage of 45 °C~60 °C

Figure 5c shows that the black paper base film rises to 60 °C within the initial 10 s after being placed on the heating plate. After that, the instantaneous temperature of the silica gel block was 31.57 °C. At the subsequent 29 s, 41 s, 119 s and 195 s, the temperature of the silica gel block was 40.30 °C, 45.03 °C, 55.05 °C and 60.11 °C, respectively. Similarly, the rate of rubber blocks rising from 30 °C to 45 °C and 60 °C is 70.8 °C/s and 15.42 °C/s, respectively. It was observed that the temperature of the rubber block rose rapidly before the initial temperature rose to 45 °C, but between 45 °C and 60 °C, the temperature rose slightly. However, compared with the base paper as the heat transfer medium, the heat transfer efficiency of black paper is obviously higher. The excellent thermal conductivity of carbon black endows the black paper base film with high thermal conductivity. Paper-based films can increase the soil temperature in a short time, inhibit the growth of weeds and meet the temperature requirements for crop growth.

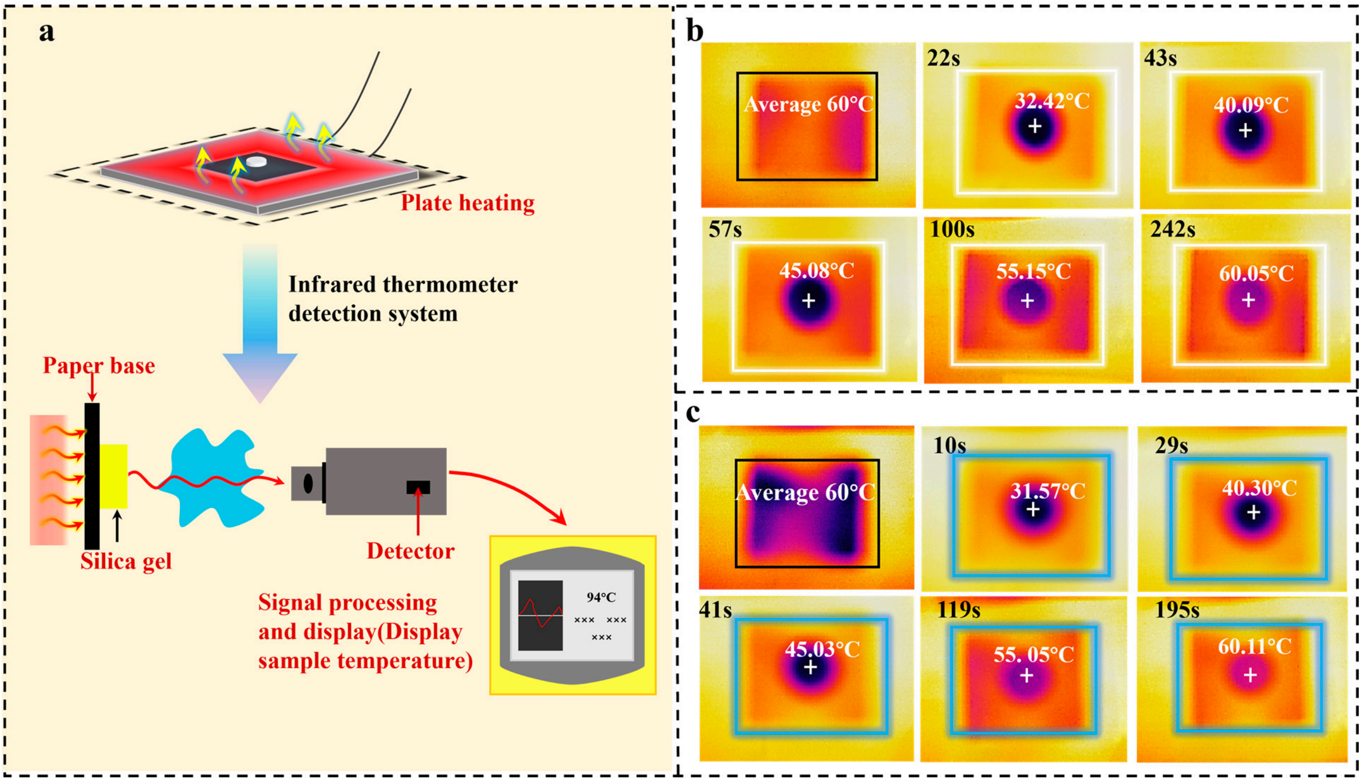

Figure 5. Study on thermal conductivity of paper base film. (**a**) Thermal conductivity experiment and schematic diagram of infrared temperature measuring gun principle; (**b**) temperature change in base film heat conduction experiment of base paper (the color shade represents the temperature change); (**c**) temperature change in heat conduction experiment of black paper base film (the color shade represents the temperature change).

3.5. Weather Resistance (UV Aging Resistance, Dry Heat Aging Resistance)

In agricultural production, the direct ultraviolet rays and the high temperature brought by sunlight are two important roles that make the plastic film naturally age, thus affecting the service life. Rainfall, direct sunlight, pulling, etc., are all natural and man-made influences that need to be considered during the use of plastic films. Therefore, the key to examine whether the paper base has weatherability is to compare whether its mechanical and hydrophobic effects have changed. Under laboratory conditions, an ultraviolet aging box and hot air aging box are used to simulate the natural environment. Hot air aging is carried out under the standard of GB/T 464-2008 [34]. Set the temperature at 150 °C for 24 h. The ultraviolet accelerated weathering test chamber is set with the radiation intensity of a fluorescent ultraviolet lamp of 0.76 $W{\cdot}m^{-2}{\cdot}nm^{-1}$ @ 340 nm and UVat (60 ± 3) °C. After that, the tensile, tear, hydrophobic and thermal conductivity of the aged paper-based samples were tested. Comparing the mechanical and hydrophobic properties of the film of base paper and black paper before and after paper aging, it is concluded that the black paper base film has excellent weather resistance, further proving the practicability of the black paper base film coated with cooked tung oil.

3.5.1. Mechanical Analysis of Weather Resistance

In Figure 6a, the black paper base film is bent upwards and downwards and twisted clockwise and counterclockwise to simulate the actual use and destruction scene on farmland. Finally, the macroscopic surface of the black paper base film remains the same. Figure 6b–d show the mechanical test for the base paper and black paper base film after ultraviolet and dry heat aging. After ultraviolet-light aging, the mechanical strength of the base paper decreased slightly. Compared with the base paper without ultraviolet aging, the maximum tensile and tearing forces of the base paper have a downward trend. On the contrary, the maximum tensile stress of the black paper-based film increased by 57.8% after ultraviolet aging. Under the irradiation of ultraviolet light, the ultraviolet light directly shines on the surface of the paper mulch film, destroying the paper fiber structure and breaking the molecular chemical bond, which leads to a significant decline in the mechanical properties of the base paper after ultraviolet aging.

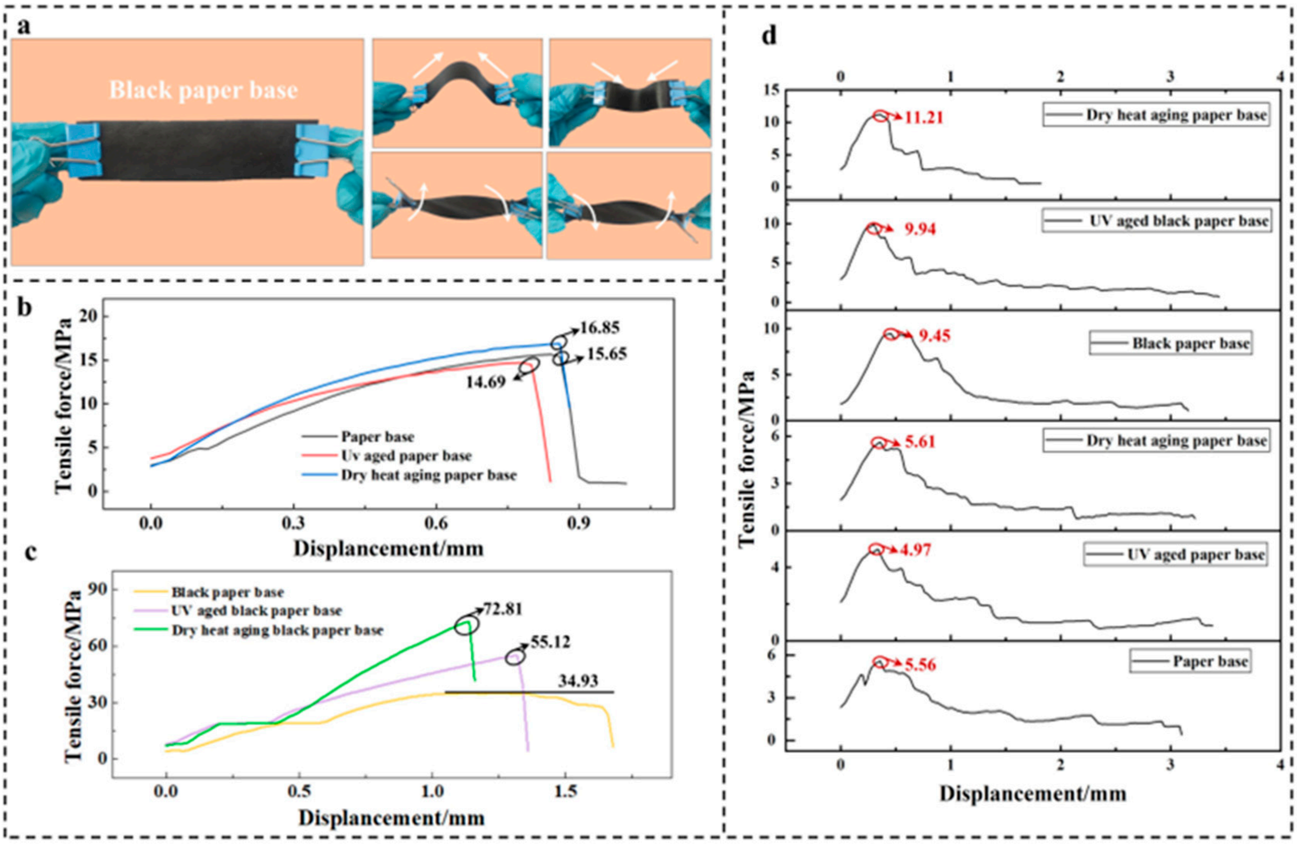

Figure 6. Weather resistance mechanical test of paper base film. (**a**) Distortion test of black paper base film (the arrow points in the direction that represents the twist of the mulch); (**b**) tensile–displacement curve of base film of base paper before and after aging; (**c**) tensile–displacement curve of black paper base film before and after aging; (**d**) tear–displacement curves of base film of base paper and black paper before and after aging.

Figure 6b–d show that the mechanical strength (tensile strength, tear strength) of the raw paper base and black paper base films is improved after dry heat aging. After dry heat aging, the maximum tensile force and tearing stress of the black base film increased by 108.5% and 18.6%, and the mechanical strength of the black base film increased even more. This is different from the ultraviolet light breaking the molecular bond structure. The aging forces the paper-based fibers to dehydrate rapidly, and the crosslinked fiber network becomes stiff, which leads to a larger external force needed to destroy the structure. In the mechanical test after dry heat aging, the mechanical strength of the black paper base film did not decrease but showed a better performance. Part of the reason is the dehydration and hardening of paper-based fibers after high-temperature treatment. The other part comes from the blessing of the oil film of cooked tung oil. Mature tung oil permeates into the inner layer of the paper base, forms an organic combination with paper fibers and the film-forming system is more stable. Compared with the original paper base, the black paper base film can effectively maintain its mechanical properties after dry and ultraviolet aging, and the small increase after ultraviolet aging and the large increase after dry and hot aging show the excellent weatherability of the black paper base film from the side.

3.5.2. Analysis of Weatherability and Hydrophobicity

The weatherability and hydrophobicity of the paper-based film were tested, and the experiment showed that the hydrophobic properties of the base film of base paper are different after ultraviolet aging and dry heat aging. The base paper aged under ultraviolet and dry heat conditions is also hydrophilic [35–41]. In the hydrophilic model in Figure 7a, the solid–liquid–gas medium θ is less than 90°, and the sample surface is wetted by droplets. When the droplets fall on the film surface of the base paper after ultraviolet and dry heat aging, the droplets will soak the base paper in a short time. Figure 7b,c show that the droplets are hydrophobic when they drop on the surface of the aged paper base, and there is a big difference in the rate at which the droplets soak into the paper base. At the same time (10 s), the UV-aged base paper was quickly soaked by droplets, and the contact angle became 57.76°. However, the dry hot aged base paper was still hydrophobic at 10 s (CA = 99.32°). This shows that UV aging and dry heat aging have different effects on the surface of a paper mulch film, and the three-dimensional rough structure of the hydrophilic paper base aged by dry heat (Figure 7g) is obviously rougher than the original paper base aged by UV (Figure 7f).

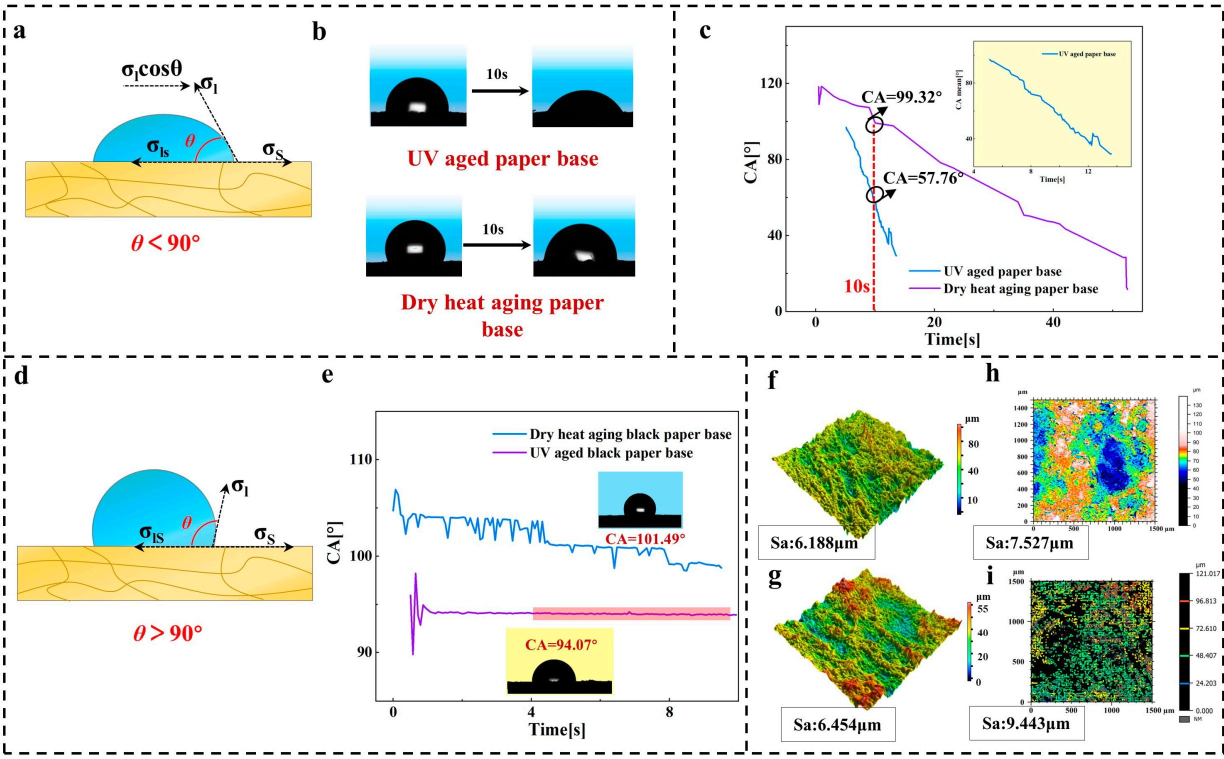

Figure 7. (**a**) Hydrophilic (CA < 90°) model; (**b**) hydrophilic infiltration process of base film of base paper after ultraviolet and dry heat aging; (**c**) contact angle curve of the base film of the base paper after ultraviolet and dry heat aging; (**d**) hydrophobic (CA > 90°) model; (**e**) contact angle of black paper base film after ultraviolet and dry heat aging (the red line highlights the stability of the contact angle value); (**f**,**g**) three-dimensional morphology of base film surface of base paper after ultraviolet and dry heat aging; (**h**,**i**) contour lines of black paper base film surface after ultraviolet and dry heat aging.

The free energy of the solid surface when a droplet drops on the solid surface is also an important factor to investigate the hydrophobic surface. The static contact angle is a basic parameter to describe the wettability of a solid surface, and the static contact angle (CA) directly reflects the wettability of a solid surface. Figure 7a,d are diagrams describing the component balance of surface tension when a liquid drop reaches an equilibrium state on a solid surface on an ideal smooth surface. Yang's equation is as follows:

$$\sigma_s = \sigma_{sl} + \sigma_l cos\theta \quad (1)$$

where σ_S represents the surface free energy (SFE) of the solid surface, σ_l represents the surface tension (SFT) of the droplet and σ_{lS} represents the interfacial tension (IFT) between the solid and the liquid. In this study, when droplets drop on the surface of a black paper-based membrane, a hydrophobic structure is formed, and the shape of droplets on the solid wall is not completely spherical because of the micro-rough structure on the surface of the black paper-based membrane and the ester group effect of cooked tung oil. We calculated the surface free energy from the contact angle and calculated the surface free energy through the Fowkes method according to Young's equation in Formula (1):

$$\sigma_{ls} = \sigma_l + \sigma_s - 2\left(\sqrt{\sigma_l^D \cdot \sigma_s^D} + \sqrt{\sigma_l^{nD} \cdot \sigma_s^{nD}}\right) \quad (2)$$

Among them, it is necessary to measure the unknown variable σ_{lS} of interfacial tension, and this is based on the surface tensions σ_S and σ_l of two phases and their interaction. The interaction between two phases is regarded as the geometric average of the dispersion force part σ^D and the non-dispersion force part σ^{nD} of the surface free energy. The surface free energy of the paper-based film before and after ultraviolet aging can be obtained by substituting σ_{lS} into Formula (1). The reliability of the preparation process of the black paper-based film was evaluated.

In the hydrophobic structure in Figure 7d, θ is greater than 90°, and the sample surface is not wetted. Figure 7e shows that the contact angle of the black paper base film after high-temperature treatment is 101.5°, which is higher than that of the unaged black paper base film by 98.9°. After ultraviolet aging, the contact angle of the black paper base is 94.0°, which still shows hydrophobicity (Figure 7h,i). Similar to the performance of the original paper base, the surface roughness of the black paper base after dry heat aging is larger than that after ultraviolet aging, and its hydrophobic performance is excellent. To sum up, the hydrophobic property of the black paper base film did not decrease significantly after ultraviolet and dry heat aging, but it still showed hydrophobicity. The coating of cooked tung oil gives the black paper base film excellent weather resistance.

3.5.3. Analysis of Weather Resistance Mechanism

The paper-based film was characterized by Fourier-transform infrared spectroscopy, and SEM and EDS were used to analyze the surface of different kinds of paper-based films. A three-dimensional surface topography instrument was used to measure the surface roughness of the paper base film and reveal the microstructure of the paper base surface. Figure 8a shows the effect mechanism of ultraviolet and dry heat aging on base paper and black paper and explains the weather resistance mechanism of the black paper base film. In the treatment process of the black paper base, cooked tung oil mainly affects the mechanical and hydrophobic properties of the black paper base film. Carbon black solution enhances its heat transfer efficiency. Soaking the paper base film coated with carbon black solution with cooked tung oil can not only fix the color but also enhance the mechanical strength, hydrophobicity and aging resistance of the black paper base film, finally achieving the effect of prolonging the service life of the paper base film. Ultraviolet light is irradiated on the surface of the black paper base film. Compared with the original paper base film, the infrared spectrum of the black paper base film after ultraviolet aging in Figure 8b has a strong amplitude peak at –CO– (lipid) (1735 cm^{-1}) and an antisymmetric stretching peak at –CH_2– (2927 cm^{-1}), and the peak is obvious. It can be seen that ripe tung oil plays an important role in maintaining the properties of paper mulch film during ultraviolet aging. Under the irradiation of ultraviolet rays, there are oxidative polymerization and free radical polymerization reactions on the surface of the black paper base, which leads to prominent wrinkles on the surface of the black paper base after the irradiation of ultraviolet rays (Figure 8d$_3$,e$_3$), showing a wrinkled membrane structure as a whole. The prominent wrinkles caused by light aging and the non-hydrophilicity of oil itself make the black paper base after ultraviolet aging still appear hydrophobic. We compared the prominent fiber profile of the base paper surface (Figure 8d$_1$,e$_1$) after UV aging. The oil film on the surface of the black paper tightly wraps the paper fiber structure, protecting the black paper base from ultraviolet light erosion.

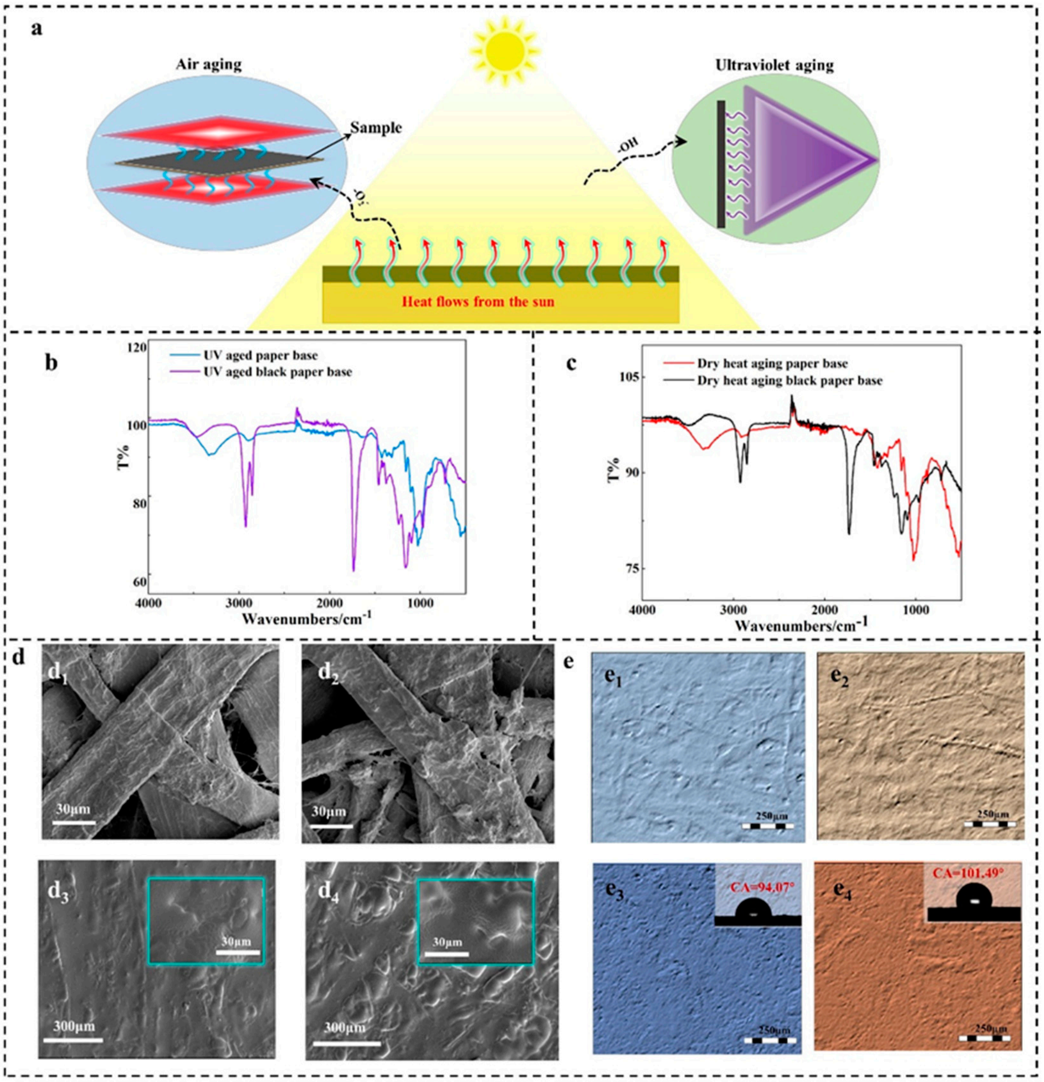

Figure 8. Analysis of weather resistance mechanism of paper base film. (**a**) Ultraviolet and dry heat aging experimental model; (**b**) infrared spectra of base paper and black paper base film after ultraviolet aging; (**c**) infrared spectra of base paper and black paper base film after dry heat aging; (**d**) SEM of base paper and black paper after UV and dry heat aging ((**d$_1$**,**d$_3$**) UV aging base paper and black paper base film, (**d$_2$**,**d$_4$**) dry heat aging base paper and black paper base film); (**e**) photo simulation of the surface of base paper and black paper after ultraviolet and dry heat aging ((**e$_1$**,**e$_3$**) ultraviolet aging base paper and black paper base film, (**e$_2$**,**e$_4$**) dry heat aging base paper and black paper base film).

Figure 8d$_4$,e$_4$ show that the cooked tung oil is dried at high temperature after the surface of the paper base is solidified, and many wrinkles are produced on the surface of the black paper base during the high-temperature treatment, causing its surface to become rougher and maintain its hydrophobic structure. The process of high heat aging is a complex oxidative polymerization reaction. Figure 8c shows that the expansion peaks of –CO– (lipid) and –CH_2– groups of black paper base after dry heat aging are more prominent.

At high temperature, the mature tung oil and oxygen molecules form more free fatty acids and a wider range of hydroxyl compounds. After accelerated aging by dry heat, trans double bonds (~972–975 cm^{-1}) are preserved in the cured structure of the cooked tung oil, and the cured structure soaked by the cooked tung oil has better mechanics and stronger resistance to dry heat aging after high-temperature treatment.

Under normal circumstances, the substance of paper will turn yellow and become brittle when exposed to sunlight for a long time, accelerating the aging of paper and shortening its service life. Obviously, conventional paper is not suitable for agricultural use. As a kind of dry oil, the black paper base film coated with cooked tung oil can still maintain its own properties and basic performance under ultraviolet irradiation and dry heat treatment, and the cooked tung oil plays a great role.

4. Conclusions

Through a simple process of spraying carbon black solution on the surface of base paper and smearing cooked tung oil on the surface, we prepared a black paper base film covered with cooked tung oil with excellent mechanical properties, hydrophobicity, high heat transfer and excellent weather resistance. The cured film of the black paper base film soaked with cooked tung oil formed a multi-dimensional network film structure, and its mechanical strength is far superior to that of base paper film; the maximum tensile force is increased by 123% compared with that of base paper. Curing the rough structure of the oil film on the surface gives the black paper a hydrophobic structure, and the contact angle reaches 97.9°. The coloring of carbon black gives the black paper base film a heat conduction effect, and the average heat transfer rate reaches 15.12 °C/s. The oil film stability system formed by the penetration of cooked tung oil into the paper base makes the black paper base film resistant to ultraviolet light and hot air. It provides a reliable basis for the feasibility of a black paper base film coated with cooked tung oil.

Author Contributions: Conceptualization, Y.W. and Y.S.; methodology, Y.W.; software, Y.Y.; validation, Y.Z. and Y.Y.; formal analysis, Y.S.; investigation, Y.S.; resources, Y.W.; data curation, Y.S.; writing—original draft preparation, Y.S.; writing—review and editing, Y.W., Y.Z. and Y.Y.; visualization, Y.Z. and Y.Y.; validation, Y.S.; supervision, Y.W.; project administration, Y.W.; funding acquisition, Y.W. All authors have read and agreed to the published version of the manuscript.

Funding: This research received no external funding.

Institutional Review Board Statement: Not applicable.

Informed Consent Statement: Not applicable.

Data Availability Statement: The raw data supporting the conclusions of this article will be made available by the authors on request.

Conflicts of Interest: The authors declare no conflicts of interest.

References

1. Wang, X.; Fan, J.; Xing, Y.; Xu, G.; Wang, H.; Deng, J.; Wang, Y.; Zhang, F.; Li, P.; Li, Z. The Effects of Mulch and Nitrogen Fertilizer on the Soil Environment of Crop Plants. *Adv. Agron.* **2019**, *153*, 121–173. [CrossRef]
2. Arora, V.K.; Singh, C.B.; Sidhu, A.S.; Thind, S.S. Irrigation, tillage and mulching effects on soybean yield and water productivity in relation to soil texture. *Agric. Water Manag.* **2011**, *98*, 563–568. [CrossRef]
3. He, Q.; Wang, J.; Wang, G.; Hao, X.; Li, A. Construction of a durable superhydrophobic flame-retardant coating on the PET fabrics. *Mater. Des.* **2023**, *233*, 112258. [CrossRef]
4. Wang, Y.; Xie, Z.; Malhi, S.S.; Vera, C.L.; Zhang, Y.; Guo, Z. Effects of gravel–sand mulch, plastic mulch and ridge and furrow rainfall harvesting system combinations on water use efficiency, soil temperature and watermelon yield in a semi-arid Loess Plateau of northwestern China. *Agric. Water Manag.* **2011**, *101*, 88–92. [CrossRef]
5. Zhou, L.; Zhang, F.; Liu, C. Improved yield by harvesting water with ridges and subgrooves using buried and surface plastic mulchs in a semiarid area of China. *Soil Tillage Res.* **2015**, *150*, 21–29. [CrossRef]
6. Qi, Y.; Beriot, N.; Gort, G.; Lwanga, E.H.; Gooren, H.; Yang, X.; Geissen, V. Impact of plastic mulch film debris on soil physicochemical and hydrological properties. *Environ. Pollut.* **2020**, *266 Pt 3*, 115097. [CrossRef]

7. Gao, H.; Yan, C.; Liu, Q.; Ding, W.; Chen, B.; Li, Z. Effects of plastic mulching and plastic residue on agricultural production: A meta-analysis. *Sci. Total Environ.* **2018**, *651*, 484–492. [CrossRef]
8. Barnes, D.; Galgani, F.; Thompson, R.C.; Barlaz, M. Accumulation and fragmentation of plastic debris in global environments. *Philos. Trans. R. Soc. Lond B Biol.* **2009**, *364*, 1985–1998. [CrossRef]
9. Brodhagen, M.; Goldberger, J.R.; Hayes, D.G.; Inglis, D.A.; Marsh, T.L.; Miles, C. Policy considerations for limiting unintended residual plastic in agricultural soils. *Environ. Sci. Policy* **2017**, *69*, 81–84. [CrossRef]
10. Miles, C.; DeVetter, L.; Ghimire, S.; Hayes, D.G. Suitability of Biodegradable Plastic Mulches for Organic and Sustainable Agricultural Production Systems. *HortScience* **2017**, *52*, 10–15. [CrossRef]
11. Harada, J.; de Souza, A.G.; de Macedo, J.R.; Rosa, D.S. Soil culture: Influence of different natural fillers incorporated in biodegradable mulching film. *J. Mol. Liq.* **2019**, *273*, 33–36. [CrossRef]
12. Brown, J.E.; Channell-Butcher, C. Black Plastic Mulch and Drip Irrigation Affect Growth and Performance of Bell Pepper. *J. Veg. Crop Prod.* **2001**, *7*, 109–112. [CrossRef]
13. Kasperbauer, M. Strawberry Yield over Red versus Black Plastic Mulch. *Crop Sci.* **2000**, *40*, 171–174. [CrossRef]
14. Anzalone, A.; Cirujeda, A.; Aibar, J.; Pardo, G.; Zaragoza, C. Effect of Biodegradable Mulch Materials on Weed Control in Processing Tomatoes. *Weed Technol.* **2010**, *24*, 369–377. [CrossRef]
15. Massenssini, A.M.; Bonduki, V.H.A.; Melo, C.A.D.; Tótola, M.R.; Ferreira, F.A.; Costa, M.D. Soil microorganisms and their role in the interactions between weeds and crops. *Planta Daninha* **2014**, *32*, 873–884. [CrossRef]
16. Portet, C.; Yushin, G.; Gogotsi, Y. Electrochemical performance of carbon onions, nanodiamonds, carbon black and multiwalled nanotubes in electrical double layer capacitors. *Carbon* **2007**, *45*, 2511–2518. [CrossRef]
17. Wang, Y.; Chen, J.; Cao, J.; Liu, Y.; Zhou, Y.; Ouyang, J.H.; Jia, D. Graphene/carbon black hybrid film for flexible and high rate performance supercapacitor. *J. Power Sources* **2014**, *271*, 269–277. [CrossRef]
18. Nadakatti, S.; Tendulkar, M.; Kadam, M. Use of mesoporous conductive carbon black to enhance performance of activated carbon electrodes in capacitive deionization technology. *Desalination* **2011**, *268*, 182–188. [CrossRef]
19. Kossyrev, P. Carbon black supercapacitors employing thin electrodes-ScienceDirect. *J. Power Sources* **2012**, *201*, 347–352. [CrossRef]
20. Song, J.P.; Tian, K.Y.; Ma, L.X.; Li, W.; Yao, S.C. The effect of carbon black morphology to the thermal conductivity of natural rubber composites. *Int. J. Heat Mass Transf.* **2019**, *137*, 184–191. [CrossRef]
21. Mishra, A.K.; Lahiri, B.B.; Philip, J. Superior thermal conductivity and photo-thermal conversion efficiency of carbon black loaded organic phase change material. *J. Mol. Liq.* **2019**, *285*, 640–657. [CrossRef]
22. Leong, C.K.; Chung, D. Carbon black dispersions as thermal pastes that surpass solder in providing high thermal contact conductance. *Carbon* **2003**, *41*, 2459–2469. [CrossRef]
23. Huang, J.; Yuan, T.; Ye, X.; Man, L.; Zhou, C.; Hu, Y.; Zhang, C.; Yang, Z. Study on the UV curing behavior of tung oil: Mechanism, curing activity and film-forming property. *Ind. Crops Prod.* **2018**, *112*, 61–69. [CrossRef]
24. Zhang, C.; Garrison, T.F.; Madbouly, S.A.; Kessler, M.R. Recent advances in vegetable oil-based polymers and their composites. *Prog. Polym. Sci.* **2017**, *71*, 91–143. [CrossRef]
25. He, Z.; Chapital, D.C.; Cheng, H.N.; Klasson, K.T.; Olanya, O.M.; Uknalis, J. Application of tung oil to improve adhesion strength and water resistance of cottonseed meal and protein adhesives on maple veneer. *Ind. Crops Prod.* **2014**, *61*, 398–402. [CrossRef]
26. Xin, Y.L.; Timar, M.C.; Varodi, A.M.; Yi, S.L. Tung oil and linseed oil as traditional finishing materials important for furniture conservation. *Pro Ligno* **2015**, *11*, 571–579.
27. Huang, Y.; Pang, L.; Wang, H.; Zhong, R.; Zeng, Z.; Yang, J. Synthesis and properties of UV-curable tung oil based resins via modification of Diels–Alder reaction, nonisocyanate polyurethane and acrylates. *Prog. Org. Coat.* **2013**, *76*, 654–661. [CrossRef]
28. Huang, Y.; Ye, G.; Yang, J. Synthesis and properties of UV-curable acrylate functionalized tung oil based resins via Diels–Alder reaction. *Prog. Org. Coat.* **2015**, *78*, 28–34. [CrossRef]
29. *GB/T22898-2008*; Paper and Board—Determination of Tensile Properties—Constant Rate of Elongation Method (100 mm/min). Standardization Administration of the People's Republic of China: Beijing, China, 2008.
30. *GB/T1040.3-2006*; Plastics—Determination of Tensile Properties—Part 3: Test Conditions for Films and Sheets. Standardization Administration of the People's Republic of China: Beijing, China, 2006.
31. Wang, S.; Yao, W.; Lu, Z.; Wang, S.; Li, B.; Liu, B. Characterization and durability assessment of fibre-reinforced tung oil lime putties for restoration. *J. Build. Eng.* **2021**, *38*, 102241. [CrossRef]
32. Samadzadeh, M.; Boura, S.H.; Peikari, M.; Ashrafi, A.; Kasiriha, M. Tung oil: An autonomous repairing agent for self-healing epoxy coatings. *Prog. Org. Coat.* **2011**, *70*, 383–387. [CrossRef]
33. Jagtap, A.R.; More, A. Developments in reactive diluents: A review. *Polym Bull.* **2022**, *79*, 5667–5708. [CrossRef]
34. *GB/T 464-2008*; Paper and Board—Accelerated Aging—Dry Heat Treatment. Standardization Administration of the People's Republic of China: Beijing, China, 2008.
35. Wang, J.; Zhang, Y.; He, Q. Stretchable superhydrophobic fluororubberfabricated by transferring mesh microstructures. *Soft Matter* **2023**, *19*, 1560. [CrossRef] [PubMed]
36. He, Q.; Ma, Y.; Wang, X.; Jia, Y.; Li, K.; Li, A. Superhydrophobic flexible silicone rubber with stable performance, anti-icing and multi-level rough structure. *ACS Appl. Polym. Mater.* **2023**, *6*, 3c00273. [CrossRef]
37. Li, A.; Wei, Z.; Zhang, F.; He, Q. A high reliability super hydrophobic silicone rubber. *Colloids Surf. A Physicochem. Eng. Asp.* **2023**, *671*, 131639. [CrossRef]

38. He, Q.; Jia, Y.; Wang, H.; He, J.; Wang, J.; Xu, Y.; Liu, Y.; Li, A. Triple conversion strategy to build anti-de-icing sheets for the leading edge of the rotor blade. *Mater. Des.* **2024**, *237*, 112516. [CrossRef]
39. He, Q.; Li, K.; Xu, Z.; Wang, J.; Wang, X.; Li, A. Research progress on construction strategy and technical evaluation of aircraft icing accretion protection system. *Chin. J. Aeronaut.* **2023**, *36*, 1–23. [CrossRef]
40. Xu, Z.; Zhang, Y.; Li, A.; Wang, J.; Wang, G.; He, Q. Research progress on compounding agent and mechanical test method of fluororubber. *J. Appl. Polym. Sci.* **2021**, *138*, 50913. [CrossRef]
41. He, Q.; Xu, Y.; Zhang, F.; Jia, Y.; Du, Z.; Li, G.; Shi, B.; Li, P.; Ning, M.; Li, A. Preparation methods and research progress of super-hydrophobic anti-icing surface. *Adv. Colloid Interface Sci.* **2023**, *323*, 103069. [CrossRef]